

Supporting Information for

Anomalously Abrupt Switching of Wurtzite-structured Ferroelectrics: Simultaneous Non-linear Nucleation and Growth Model

Keisuke Yazawa^{1,2*}, John Hayden³, Jon-Paul Maria³, Wanlin Zhu³, Susan Trolier-McKinstry³, Andriy Zakutayev¹, Geoff L. Brenneka^{2*}

*Corresponding authors: Email: Keisuke.Yazawa@nrel.gov; geoff.brenneka@mines.edu

Supplementary Figures

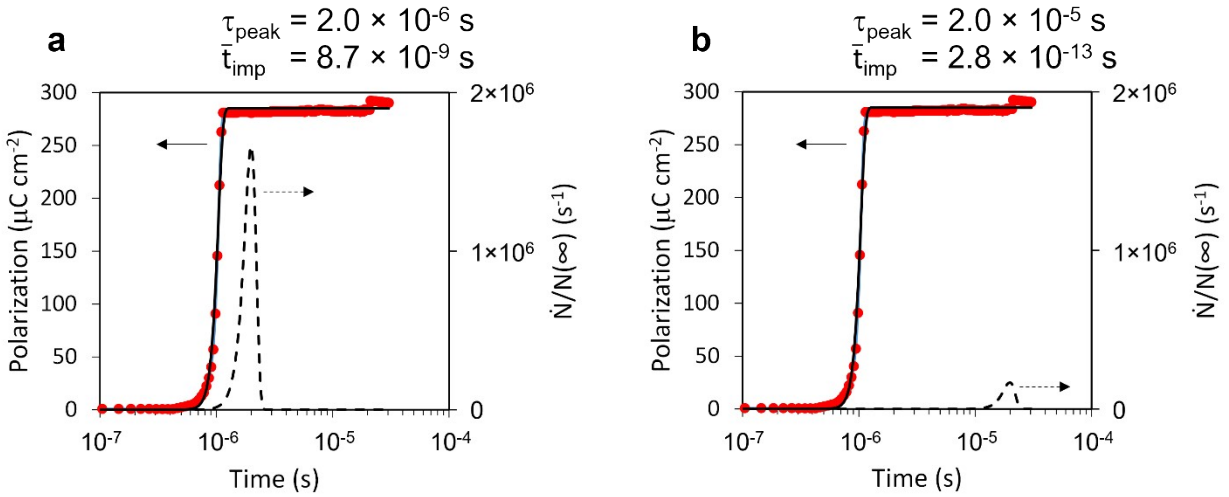


Fig. S1. Fitting results with the extended KAI model. Black line is the simulated curve, and red circles are the experimental results for $\text{Al}_{0.94}\text{B}_{0.06}\text{N}$ (a) selected faster nucleation rate ($\tau_{\text{peak}} = 2 \times 10^{-6} \text{ s}$) and (b) selected slower nucleation rate ($\tau_{\text{peak}} = 2 \times 10^{-5} \text{ s}$). Both the simulated curve fit well with the experimental results with the optimal domain wall velocities or average impingement time; impingement time of the fast nucleation rate simulation is faster than that of slow nucleation rate simulation. Thus, the τ_{peak} and \bar{t}_{imp} values using the model have a fittable range.

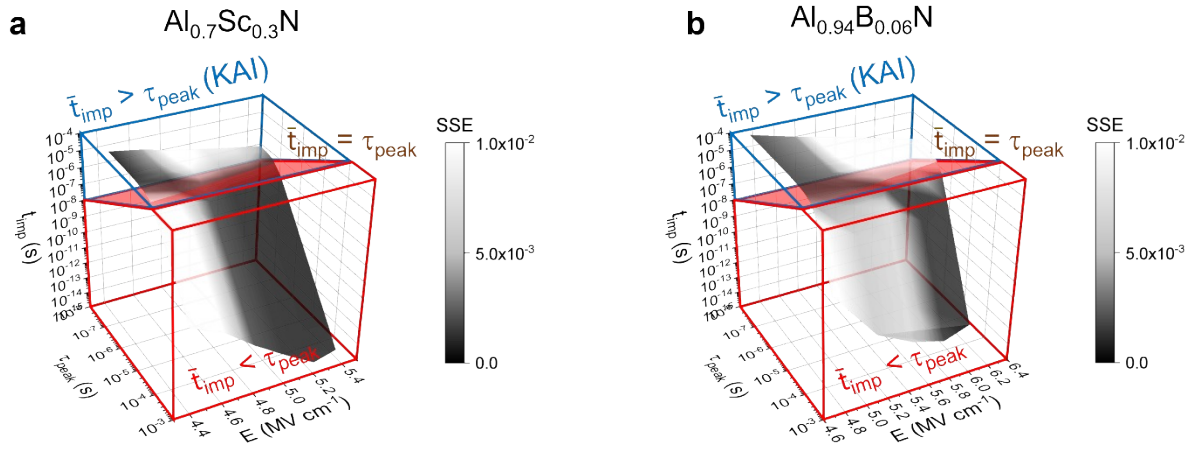


Fig. S2. Fitting quality map as a function of fitting parameters. The sum of squares of error (SSE) for fitting the $t_{\text{peak}} - t_{\text{imp}} - E$ surface is represented with the depth of gray scale, with darker regions representing better fits. (a) Fitted $t_{\text{peak}} - t_{\text{imp}} - E$ surface shaded according to SSE for $\text{Al}_{0.7}\text{Sc}_{0.3}\text{N}$ and (b) for $\text{Al}_{0.94}\text{B}_{0.06}\text{N}$. The red-colored plane (seen nearly edge-on in both plots) represents $t_{\text{peak}} = t_{\text{imp}}$, and low SSE (well fitted) conditions pass across the plane with varying electric field for both materials.

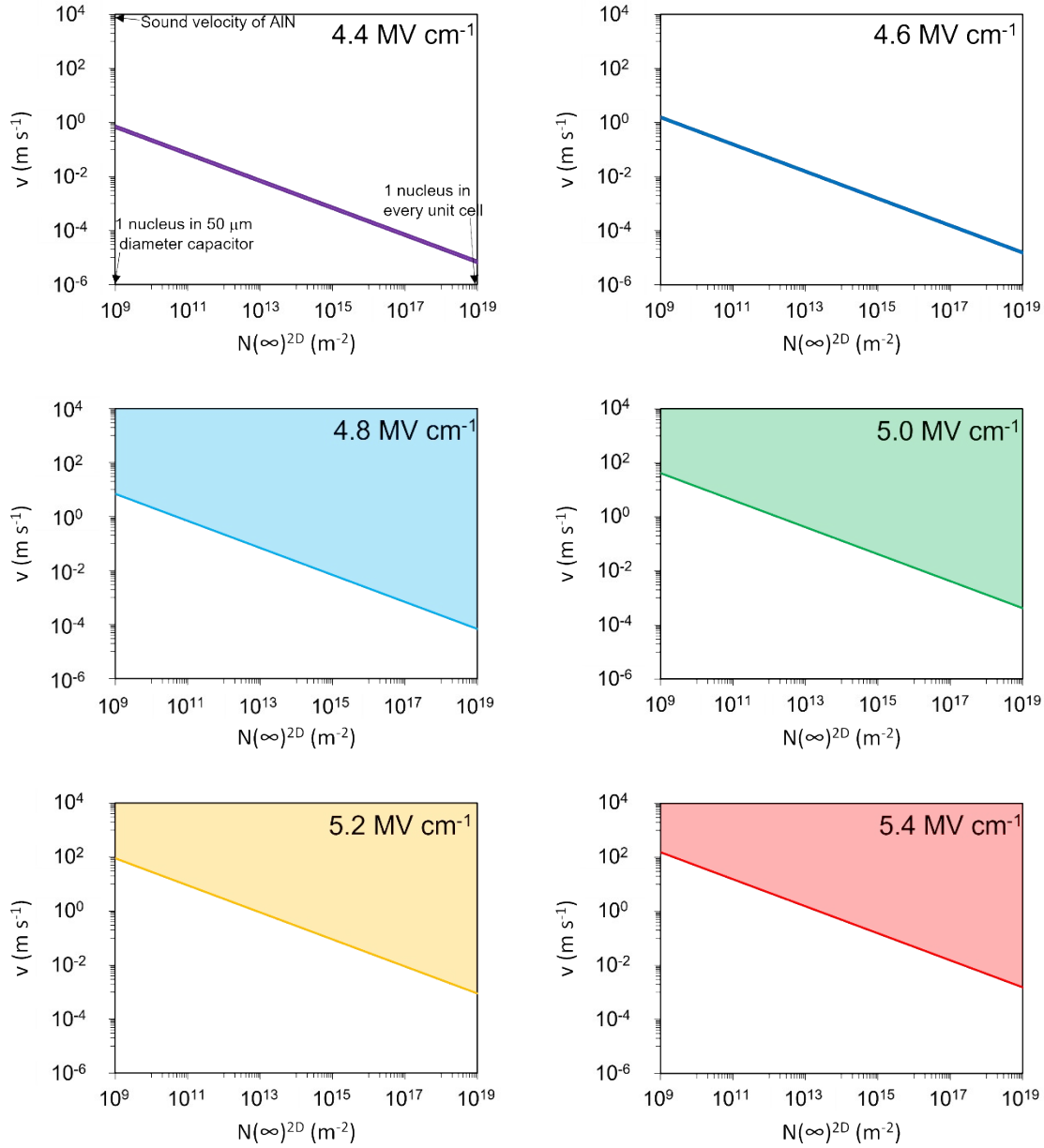


Fig. S3. Domain wall velocity of $\text{Al}_{0.7}\text{Sc}_{0.3}\text{N}$ as a function of saturated nucleation densities $N(\infty)^{2D}$ for various electric fields, $4.4 \text{ MV cm}^{-1} \sim 5.4 \text{ MV cm}^{-1}$. The shaded region represents the possible range due to the range of the fitted $\bar{\tau}_{\text{imp}}$ or $vN(\infty)^{1/2}$. The saturated nucleation densities limited to the practical range from one nucleus for the measured device size to one nucleus for each unit lattice. The velocity range shown is up to the sound velocity of AlN. Physically reasonable velocities for the domain wall exist independent of the nucleation density assumed.

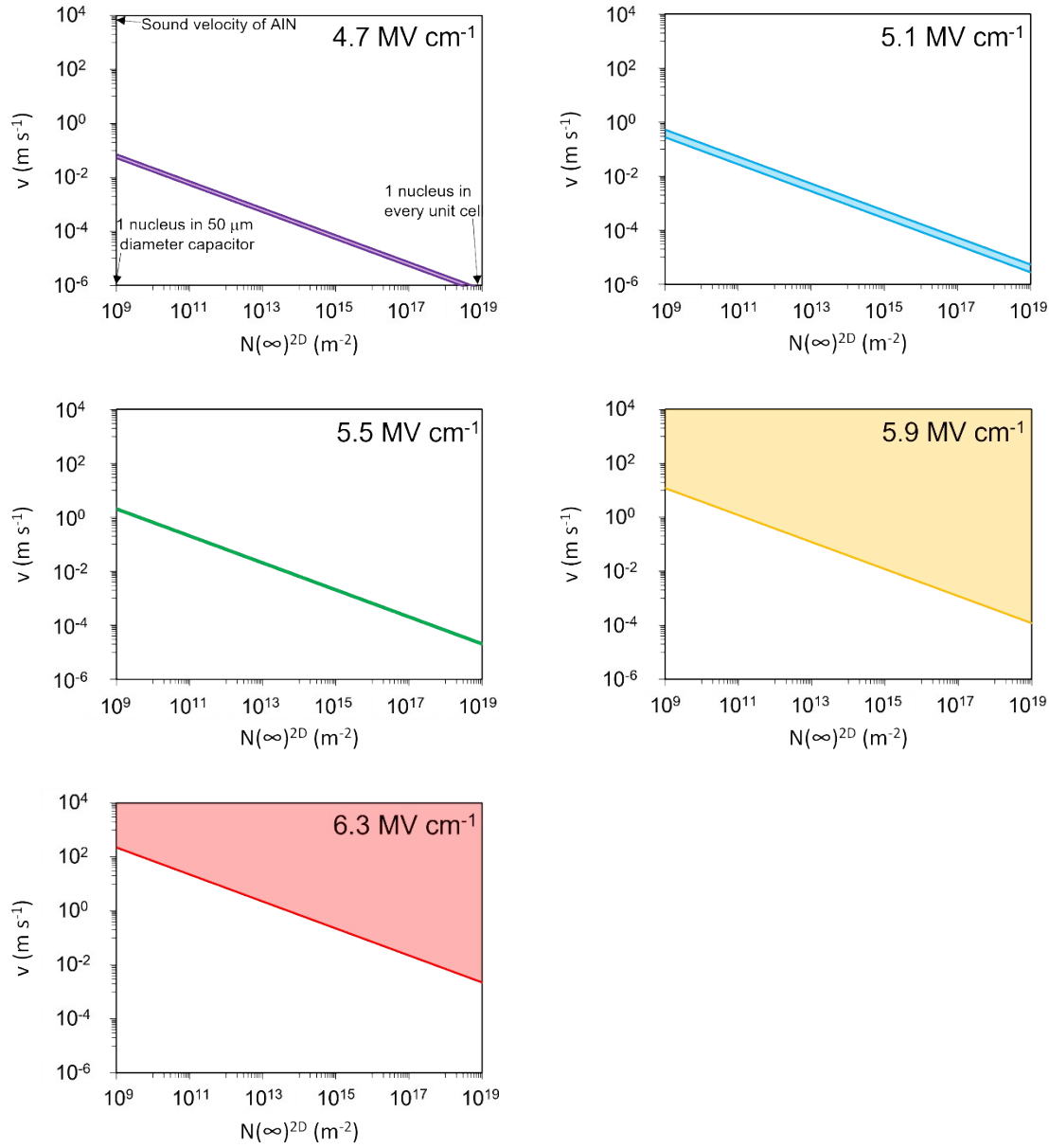


Fig. S4. Domain wall velocity of $\text{Al}_{0.94}\text{Sc}_{0.06}\text{N}$ as a function of saturated nucleation densities $N(\infty)^{2D}$ for various electric fields, $4.7 \text{ MV cm}^{-1} \sim 6.3 \text{ MV cm}^{-1}$. The shaded region represents the possible range arising from the fitted \bar{v}_{imp} or $vN(\infty)^{1/2}$. The saturated nucleation densities shown are limited to the range from one nucleus per measured capacitor to one nucleus for each unit lattice. The velocity is plotted up to the sound velocity of AlN. Physically reasonable domain wall velocities exist for all plausible nucleation densities.

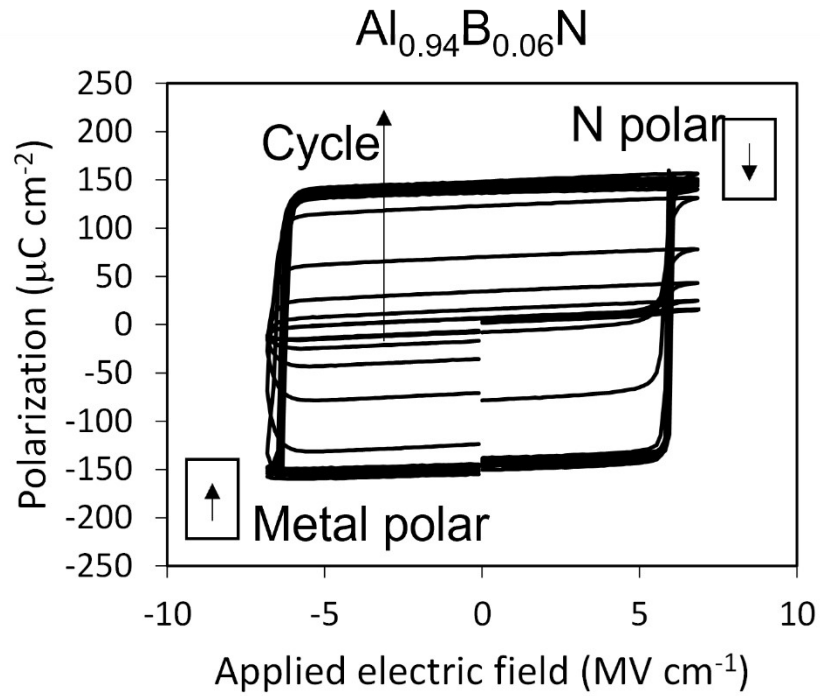


Fig. S5. P-E hysteresis loop with wakeup behavior on wurtzite-structured $\text{Al}_{0.94}\text{B}_{0.06}\text{N}$ film, showing the significant wakeup behavior. The hysteresis loops are taken under a repeated triangular excitation field (6.9 MV cm^{-1} and 10 kHz).

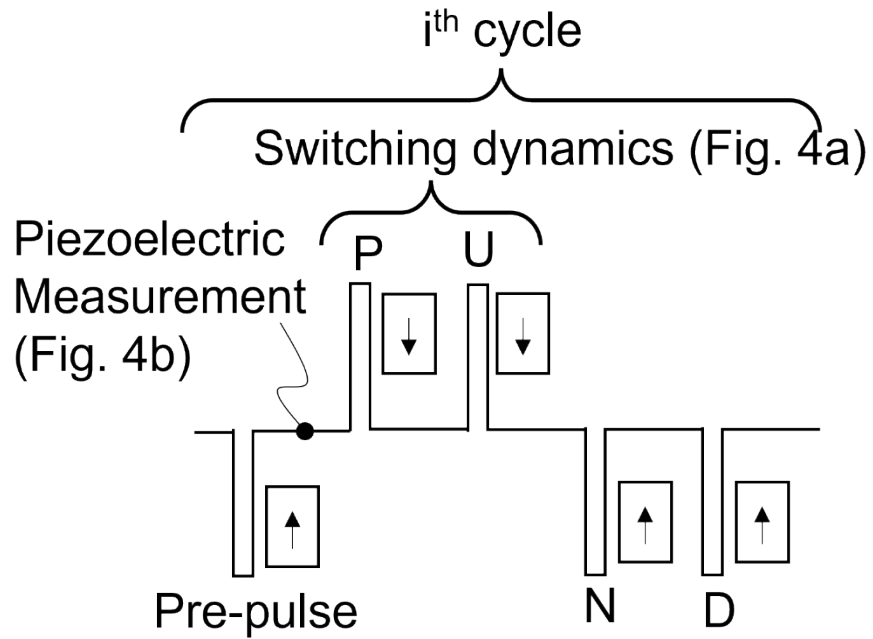


Fig. S6. Pulse sequence for cycling dependence of switching dynamics and piezoelectric property. The piezoelectric property taken prior to P pulse represents state just prior to the switching dynamics measurements.

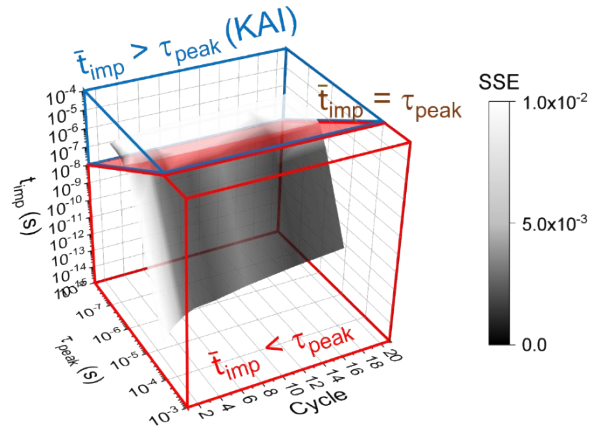


Fig. S7. Fitting quality map as a function of fitting parameters. The sum of squares of error (SSE) for fitting the $t_{\text{peak}} - \bar{t}_{\text{imp}} - \text{cycle}$ surface is represented with the depth of gray scale for $\text{Al}_{0.94}\text{B}_{0.06}\text{N}$, with darker regions representing better fits. The red-colored plane (seen nearly edge-on in both plots) represents $\tau_{\text{peak}} = \bar{t}_{\text{imp}}$, and low SSE (well fitted) conditions pass across the plane with varying number of cycles.

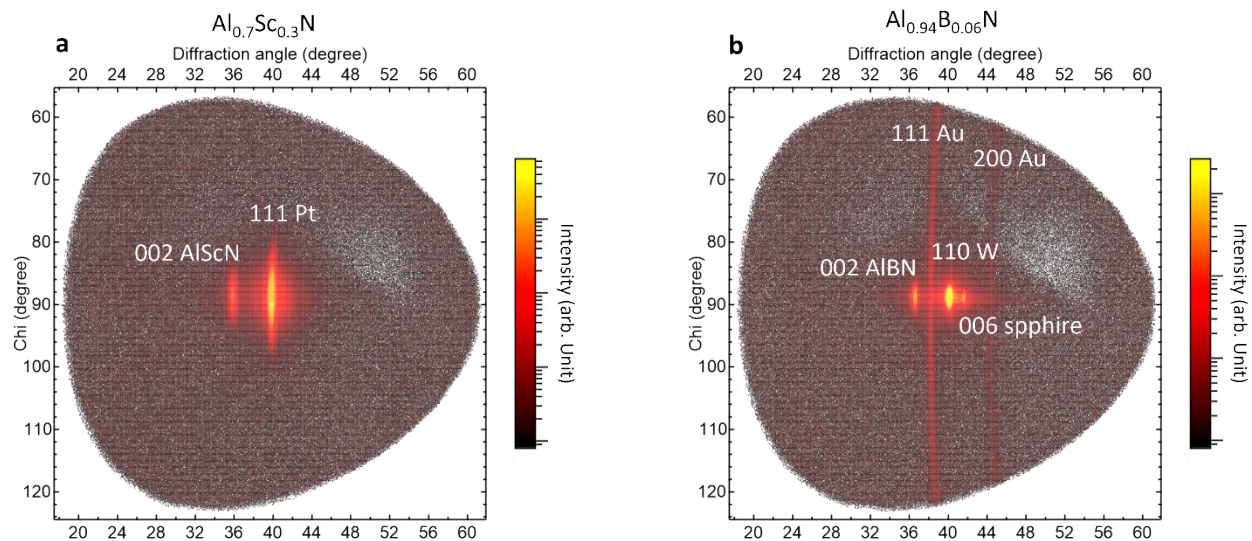


Fig. S8. 2D (2θ-chi) diffraction scan for (a) $\text{Al}_{0.7}\text{Sc}_{0.3}\text{N}$ and (b) $\text{Al}_{0.94}\text{B}_{0.06}\text{N}$ films. The diffraction patterns of both films show 002 textured wurtzite phase without any secondary crystalline phase or orientation. Chi 90 degree represents the surface normal direction.